Macromolecules

Article

pubs.acs.org/Macromolecules

Order−Order Transition between Equilibrium Ordered Bicontinuous Nanostructures of Double Diamond and Double Gyroid in Stereoregular Block Copolymer

Che-Yi Chu,[†] Wen-Fu Lin,[‡] Jing-Cherng Tsai,[‡] Chia-Sheng Lai,[†] Shen-Chuan Lo,[§] Hsin-Lung Chen,*[,†] and Takeji Hashimoto*[,†,⊥]

[†]Department of Chemical Engineering and Frontier Research Center on Fundamental and Applied Sciences of Matters, National Tsing Hua University, Hsin-Chu 30013, Taiwan

[‡]Department of Chemical Engineering, National Chung Cheng University, Chia-Yi 62102, Taiwan

[§]Material and Chemical Research Laboratories, Industrial Technology Research Institute, Chutung, Hsin-Chu, Taiwan

[⊥]Advanced Science Research Center, Japan Atomic Energy Agency, Naka-gun, Ibaraki Pref. 319-1195, Japan

Supporting Information

ABSTRACT: While ordered bicontinuous double diamond (OBDD) in block copolymers has always been considered as an unstable structure relative to ordered bicontinuous double gyroid (OBDG), here we report the existence of a thermodynamically stable OBDD structure in a diblock copolymer composed of a stereoregular block. A slightly asymmetric syndiotactic polypropylene-*block*-polystyrene (sPP-*b*-PS) as cast from xylene was found to display the OBDD morphology. When the OBDD-forming diblock was heated, this structure transformed to the OBDG phase at ca. 155 °C. Interestingly, OBDD was recovered upon cooling even in the temperature range above melting point of sPP, indicating that OBDD was a thermodynamically stable structure for sPP-*b*-PS melt, which was in contradiction to the conventional view. We propose that the larger free energy cost encountered in OBDD due to the larger packing frustration may be compensated sufficiently by the release of free energy due to local packing of the conformationally ordered segments of sPP blocks, which stabilizes the OBDD structure at the lower temperatures.

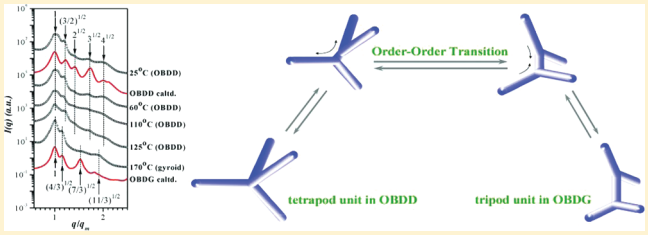

INTRODUCTION

Block copolymers have attracted great attention because of their capability of self-assembling into a series of long-range ordered nanostructures according to the block composition.[1] The lamellar and hexagonally packed cylindrical nanostructures constructed by block copolymers have been extensively used as nanoporous structure-directing agents,[3,2] templates for 1-D and 2-D photonic band gap materials,[4,5] and masks for nanolithography.[7−6] However, the nanopatterns translated from these nanostructures exhibit structural features such as low spatial continuity and less sustainability owing to the isolated microdomains. To reinforce further the potential application of block copolymers, the ordered bicontinuous structure, such as the double gyroid (OBDG) phase,[9] was introduced to fabricate nanostructured networks,[10,11] 3-D photonic crystals,[12] bulk heterojunction solar cells,[13,14] and low-refractive-index materials.[15]

The present study reports the existence of another thermodynamically stable bicontinuous structure, i.e., ordered bicontinuous double diamond (OBDD), in a diblock copolymer composed of a stereoregular block. Moreover, we clarify that the OBDD structure formed in this system underwent a thermally reversible transition to or from the OBDG phase upon heating or cooling, respectively, thereby representing the first instance of thermally induced order−order transition between the thermodynamically equilibrium bicontinuous structures of block copolymers. OBDD is constructed by 4-fold nodes connected with $Pn\bar{3}m$ symmetry and (6,4) nets.[16,17] This structure is different from OBDG, which is constructed by 3-fold nodes connected with $Ia\bar{3}d$ symmetry and (10,3) nets.[9] In complex fluids such as surfactants,[18] OBDD is known to be more common than OBDG within certain parameter space. However, the OBDD structure has always been considered to be unstable relative to OBDG for conventional block copolymers with van der Waals interactions only. The stability of OBDD relative to lamellae, OBDG, hexagonally packed cylinders, and bcc-packed spheres has been studied by theoretical calculations.[19−21] None of these studies provided a theoretical basis for considering OBDD as a thermodynamically stable structure in strongly segregated block copolymers. In the weakly segregated systems, the calculated

Received: September 9, 2011
Revised: December 11, 2011
Published: March 1, 2012

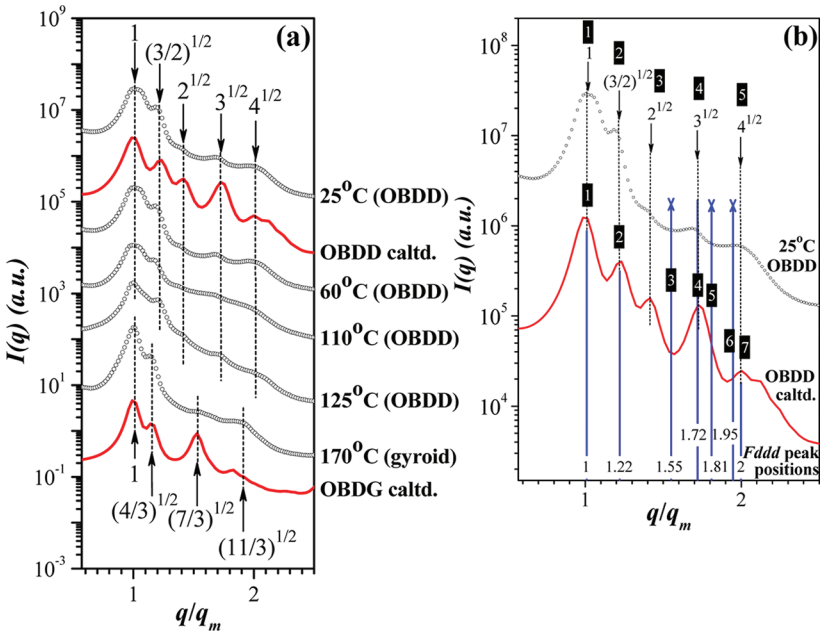

Figure 1. (a) Temperature-dependent SAXS profiles of the as-cast sPP-*b*-PS films obtained in a heating cycle, where each profile was collected after annealing at each temperature for 5 min, and followed by data acquisition for 5 min. The red solid curves represent the calculated SAXS curves of the OBDD and OBDG structures. The scattering profiles are presented as a function of q/q_m, with q_m being the position of the primary peak at each temperature. (b) Comparison of the peak-position ratios between the OBDD and *Fddd* structures. Blue lines indicate the peak-position ratios of *Fddd*.

free energy of OBDD was also never lower than that of OBDG.[22−24]

The issue regarding why OBDG is more stable than OBDD can be considered by the following two thermodynamic factors: (1) the interfacial free energy that favors the structure having the least interfacial area per unit volume[25] and (2) the packing frustration that favors microdomains with uniform thicknesses because the block chains do not have to be stretched excessively to fill space uniformly to attain the normal liquid density.[26] The calculated interfacial shape of OBDG has a lower standard deviation from the constant mean curvature (CMC) surface compared to that of OBDD; therefore, OBDG is more stable than OBDD in terms of minimization of packing frustration. This postulate was supported from the self-consistent mean-field theory (SCFT) calculations for the blends of A-*b*-B with homopolymer A (h-A), where the addition of h-A to the minority domains in the blend preferentially filled the space in the center of A domains, thereby relieving the packing frustration and stabilizing the OBDD structure over a very narrow range of composition.[26,27] Although both theoretical and experimental studies have predicted or reported the existence of the OBDD phase in A-*b*-B/h-A blends, the order−order transition (OOT) between equilibrium OBDD and OBDG has never been found thus far.

In this study, we disclose the formation of the OBDD morphology in the solvent-cast film of a slightly asymmetric diblock copolymer composed of a stereoregular block, syndiotactic polypropylene (sPP), and a conventional coil block, polystyrene (PS). This OBDD structure transformed to the OBDG phase upon heating the sPP-*b*-PS to ca. 155 °C, and the OBDG structure transformed back to OBDD on subsequent cooling even in the temperature range above melting temperature of sPP. The thermal reversibility of the morphological transformation indicated that OBDD is an equilibrium structure in the present diblock system. The stability of the OBDD phase in the present diblock melt will be discussed on the basis of the relief of the free energy cost of the packing frustration by local packing of conformationally ordered segments of sPP blocks in the melt, a new physical factor brought about by the stereoregularity of the block chain. Our finding presents a new scenario that the introduction of stereoregularity into the constituting block may release the packing free energy of diblock chains in the microdomain space, which in turn stabilizes the otherwise unstable nanostructure.

EXPERIMENTAL SECTION

Materials and Sample Preparation. The sPP-*b*-PS diblock copolymer ($M_{n,sPP}$ = 6800, $M_{n,PS}$ = 9400, PDI = M_w/M_n = 1.19) studied here was prepared in two steps according to the procedure reported in the literature.[28] First, 4-methylstyrene-capped sPP (M_n = 6800, PDI = 1.32), which served as an end-functionalized prepolymer, was prepared by syndiospecific polymerization of propylene conducted in the presence of 4-methylstyrene and hydrogen using $Me_2C(Cp)$-(Flu)$ZrCl_2$ as the catalyst. Second, the 4-methylstyrene-capped sPP was converted into silyl chloride-capped sPP, which was in situ treated with living anionic polystyrene (M_n = 9400 g/mol, PDI = 1.02) to yield the sPP-*b*-PS (the detailed synthetic and purification methods for sPP-*b*-PS can be found in the literature[28]). Figure S1 of the Supporting Information shows the ^{1}H NMR spectrum of the resulting sPP-*b*-PS. The successful preparation of a structurally well-defined sPP-*b*-PS sample can be further elucidated by the GPC analysis shown in Figure S2 (in the Supporting Information), which compares the GPC elution curves of the 4-methylstyrene-capped sPP (M_n = 6800, M_w/M_n = 1.32) and the living anionic polystyrene (M_n = 9400 g/mol, M_w/M_n = 1.02) with that of the sPP-*b*-PS (M_n = 16200 g/mol, M_w/M_n = 1.19). The symmetric GPC elution curve observed for the block copolymer rules out the possibility of the homopolymer contamination. The volume fraction of sPP block in this sample was 0.46 in the melt state.[29]

For the film preparation, the diblock copolymer was dissolved in xylene solvent at 50 °C, and the solution was subsequently cast on the Petri dish. The film was obtained after evaporating most of the solvent

quickly on the hot plate at ca. 140 °C (≅ boiling point of xylene). The film was further annealed at 100 °C (>T_g^{PS}) for 1 h followed by drying in vacuum at 70 °C for 24 h.

Small-Angle X-ray Scattering (SAXS) Measurement. The morphology of the sPP-*b*-PS was probed by SAXS performed at the Endstation BL23A1 of the National Synchrotron Radiation Research Center (NSRRC), Taiwan. The energy of X-ray source and the sample-to-detector distance were 8 keV and 1815 mm, respectively. The scattering signals were collected by a MarCCD detector of 512 × 512 pixel resolution. For the structure characterization, the sample was equilibrated at each temperature for 5 min followed by data acquisition for 5 min. The scattering intensity profile was output as the plot of the scattering intensity (I) vs the magnitude of the scattering vector, $q = (4\pi/\lambda)\ \sin(\theta/2)$ (θ = scattering angle). The SAXS profiles were corrected for the incident beam intensity, the detector sensitivity, and the background arising from the thermal diffuse scattering (TDS).

Fourier Transform Infrared Spectroscopy (FTIR) Measurement. The infrared spectra were recorded at a resolution of 1 cm^{-1} over 32 scans on a Nicolet AVATAR 320 FTIR spectrometer under a nitrogen atmosphere. The sPP-*b*-PS was cast directly onto a KBr pellet. The films were thin enough to be within the absorbance range where the Beer−Lambert law is obeyed. For the molecular conformation characterization, the sample was equilibrated at each temperature for 5 min prior to data acquisition.

RESULTS AND DISCUSSION

The theoretical scattering profiles of the OBDD and OBDG phase calculated by assuming *Pn*3*m* and *Ia*$\bar{3}$*d* space group symmetry, respectively, with the 3D network domain structure are shown in Figure 1a (the entire scattering profiles are shown in Figure S3 of the Supporting Information). The algorithm and model adopted were developed by Förster et al.,[33] which took into account the domain size distribution, distortion of domain spacing, grain size, and peak shape which varied analytically between Lorentzian and Gaussian functions. The OBDD structure exhibits a series of diffraction peaks with position ratio of $1:(3/2)^{1/2}:2^{1/2}:3^{1/2}:4^{1/2}$, corresponding to (110), (111), (200), (211), and (220) planes, respectively. The OBDG structure displays four diffraction peaks with position ratio of $1:(4/3)^{1/2}:(7/3)^{1/2}:(11/3)^{1/2}$, corresponding to (211), (220), (321), and (332) planes, respectively. The obvious difference between the position of the second-order peak relative to that of the primary peak (i.e., $(3/2)^{1/2}$ = 1.22 for OBDD vs $(4/3)^{1/2}$ = 1.15 for OBDG) can be used as the main index to distinguish these two structures from the SAXS profile.

Figure 1a also shows the temperature-dependent synchrotron-SAXS profiles of sPP-*b*-PS obtained in the heating process of the as-cast film (the entire scattering profiles are shown in Figure S4 of the Supporting Information), where each profile was collected after annealing at each temperature for 5 min, followed by data acquisition for 5 min. The scattering profiles are presented as a function of q/q_m, with q_m being the position of the primary peak (see Table 1) for clear identification of the change of the relative peak positions with temperature. The SAXS profile observed at 25 °C showed five peaks; the ratios of the higher-order peak positions to the primary peak position were not integral, indicating that the diblock did not exhibit lamellar morphology in spite of its rather symmetric composition. The observed peak-position ratios were indeed consistent with that predicted by the OBDD structure (the red curve).[33] The relative intensities of the observed peaks also agreed quite well with those of the calculated profile except for the fourth-order peak. This discrepancy may be attributed to the approximation of the form factor of the building block by the cylindrical form factor in calculating the theoretical SAXS pattern. When the copolymer was heated to 170 °C, the position of the second-order peak relative to that of the first-order peak shifted clearly from $(3/2)^{1/2}$ to $(4/3)^{1/2}$, and the scattering pattern became consistent with that associated with the OBDG phase. Therefore, a phase transition from OBDD to OBDG occurred upon the heating.

Table 1. Value of the Position of the Primary Peak (q_m) in Figure 1

T (°C)	25	60	110	125	170
q_m (nm^{-1})	0.26	0.26	0.26	0.25	0.27

The observed SAXS profiles at the low temperatures $T \leq 125$ °C were identified as the scattering from the OBDD symmetry with 4-fold nodes rather than the OBDG symmetry with 3-fold nodes, judging from the fact that the observed peak-position ratios matched with those predicted by the OBDD structure much better than those predicted by the OBDG phase. Since another ordered bicontinuous structure, *Fddd*, also has 3-fold nodes,[34] it is important to clearly distinguish the OBDD structure from the *Fddd* structure. For this purpose, the observed peak position ratios were further compared with those associated with the orthorhombic *Fddd* phase exhibiting the scattering peak position ratio of 1:1.22:1.55:1.72:1.81:1.95:2.00, etc.,[34] as shown by the solid blue vertical lines in Figure 1b. Except for the second-, fourth-, and seventh-order peaks (i.e., q/q_m = 1.22, 1.72, and 2) of the *Fddd* structure which were close to the observed second-, fourth-, and fifth-order peaks of OBDD, the third-, fifth-, and sixth-order ones (i.e., q/q_m = 1.55, 1.81 and 1.95) of *Fddd* were not identified in our observed SAXS profile. Moreover, the observed third-order peak at $q/q_m = 2^{1/2}$ is unidentified by *Fddd* but identified by OBDD. Consequently, we ruled out the formation of *Fddd* structure in the present diblock copolymer as well as the order−order phase transition from OBDD to *Fddd* as an order−order transition from 4-fold nodes to 3-fold nodes.

Since the equilibration time at each temperature was short in the synchrotron SAXS experiment despite the higher resolution for the scattering peaks, we conducted an in-house SAXS measurement to examine the thermodynamic stability of the phases and the thermal reversibility of the phase transition with much longer equilibration time at each temperature. Figure 2 shows the temperature-dependent SAXS profiles (focused on the first four scattering peaks) taken with the in-house SAXS measurements of the as-cast sPP-*b*-PS (the entire scattering profiles are shown in Figure S5 of the Supporting Information), where the sample was annealed at each temperature for 30 min followed by data acquisition for 1 h. Similar to that found in Figure 1, the as-cast sample exhibited the OBDD structure as evidenced by the scattering profile having a series of the peaks at the relative peak positions of $1:(3/2)^{1/2}:2^{1/2}:3^{1/2}:4^{1/2}$.

The OBDD structure experienced, to some extent, structural rearrangement caused by the melting of sPP crystallites (T_m^{sPP} ≅ 124 °C, the peak temperature of the melting endotherm; see the DSC thermogram in Figure S6 of the Supporting Information) and the gains of mobility of PS blocks and junction points upon heating to 110−135 °C, as manifested by the broadening of the scattering peaks. However, the scattering peaks of the OBDD structure became sharp and narrow again at $T \geq 140$ °C, where the effect of sPP crystallization completely disappeared (T_{mh}^{sPP} = 137 °C, the end temperature of melting of sPP crystallites; see the DSC thermogram in Figure S6). This result clarifies that the formation of the OBDD

dx.doi.org/10.1021/ma202057g | *Macromolecules* 2012, 45, 2471−2477

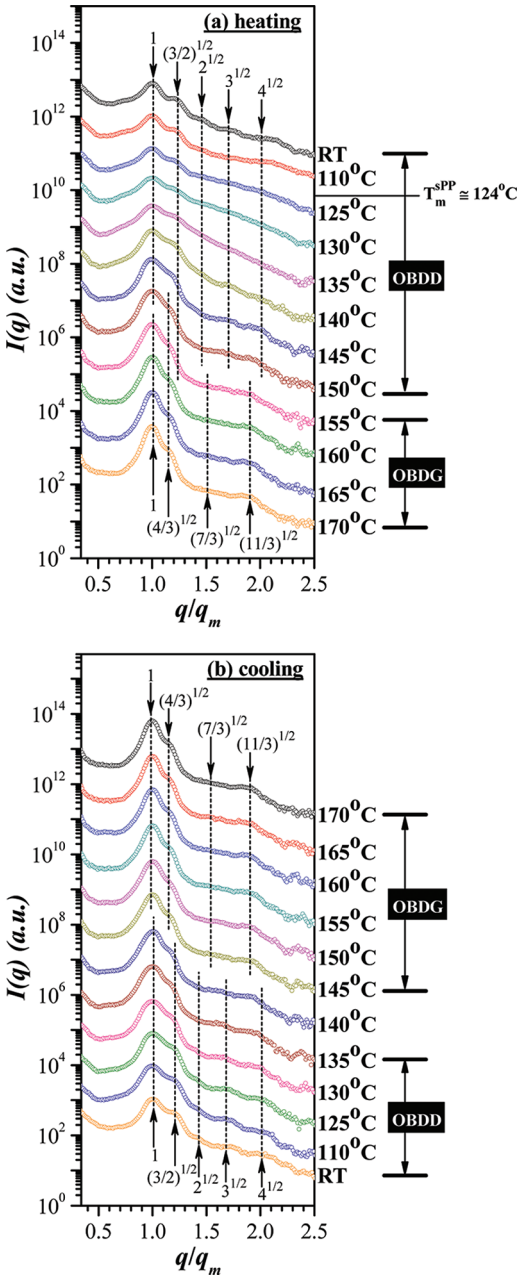

Figure 2. Temperature-dependent SAXS profiles of the as-cast sPP-*b*-PS: (a) a heating cycle and (b) a cooling cycle. Each profile was collected after annealing at each temperature for 30 min and followed by data acquisition for 1 h. The scattering profiles are presented as a function of q/q_m with q_m being the position of the primary peak at each temperature.

phase was not driven by the crystallization of sPP block. Upon further heating, a phase transition from the OBDD to OBDG structure took place between 150 and 155 °C. It is worth mentioning that both the OBDD and OBDG structures may coexist at 150 ≤ T (°C) < 155, possibly due to effects of random thermal noise, as in the case of the order-disorder coexistence in the very narrow temperature range around the order-disorder transition temperature,[35-37] and/or the kinetic effect (the slow transition). The latter effect is due to a very small degree of the superheating and supercooling from OOT in this temperature range. Interestingly, the OBDG structure transformed back to the OBDD structure upon subsequent cooling, as shown in Figure 2b. The thermal reversibility of the OOT attested that OBDD was the stable structure at the low temperatures. The OBDD structure became more ordered in the cooling process comparing with that found in the heating due to being less influenced by the crystallization of sPP.

The temperature dependence of the inverse of the primary scattering peak intensity (I_m^{-1}) above T_m^{sPP} is displayed in Figure 3. The peak intensity significantly increased at 125−140

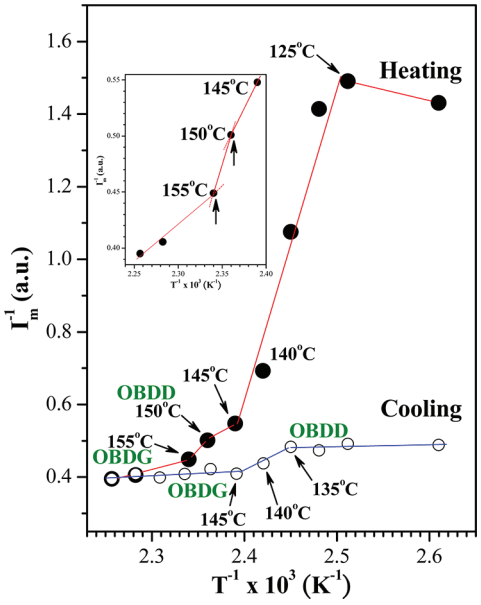

Figure 3. Temperature dependence of the inverse of the intensity of the primary scattering peak (I_m^{-1}) for the heating process of the as-cast sPP-*b*-PS and the subsequent cooling process. The inset shows the enlarged plot for the temperature ranging from 145 to 170 °C in the heating process.

°C in the heating process due to an increasing degree of ordering of the OBDD structure upon the melting of sPP crystallites. Contrarily, the intensity of scattering peak below 135 °C ($<T_{mh}^{sPP}$ = 137 °C) in the cooling process almost remained constant, due to pinning of the ordering process of OBDD via sPP crystallization. The large hysteresis in the temperature between 125 and 135 °C was attributed to the melting/crystallization of sPP blocks.

Let us further examine the data above T_{mh}^{sPP} where the kinetic effects of crystallization/melting were small or excluded. The transitions from OBDD to OBDG and OBDG to OBDD were clearly characterized by the discontinuity in I_m^{-1} in the heating (150−155 °C shown in the inset) and cooling (145−135 °C) process, respectively. A hysteresis was also found when comparing the peak intensity I_m in the heating and cooling process across the OOT. Both the discontinuity and the hysteresis observed here revealed that the order−order transition was the first-order phase transition in nature. These results evidenced that OBDD and OBDG were both thermodynamically stable structures in this system.

The stability of the OBDD structure was further demonstrated by a long-time annealing of the OBDD-forming sample to examine if the OBDD phase would transform into another more stable structure upon the annealing. Here the SAXS profile of sPP-*b*-PS was measured at room temperature after the sample has been isothermally annealed at 140 °C for 24 h, followed by quenching to liquid nitrogen to freeze the structure

dx.doi.org/10.1021/ma202057g | *Macromolecules* 2012, 45, 2471−2477

formed at 140 °C (see Figure S7 of the Supporting Information). It is obvious that the scattering profile still matched well with that prescribed by the OBDD phase, showing that OBDD in sPP-*b*-PS diblock copolymers is a stable structure.

To observe the OBDD structure in real space, the annealed sample was cut into the ultrathin section for observations under transmission electron microscopy (TEM). The formation of OBDD phase was evidenced by the micrograph displayed in Figure S8 of the Supporting Information, showing the image of the rhombus pattern. As indicated by Hasegawa et al.,[17] the projection from the [100] direction of a double-diamond (DD) lattice would give rise to a square-lattice image (see Figure S8 of the Supporting Information). The rhombus lattice image observed here should arise from a slight tilt of such a square lattice. The slight tilt made the projection vector slightly deviate from the [100] direction, so that the sequentially connected rods with an inclined angle were projected as an undulation pattern as observed in the image.

Our SAXS results have thus revealed the occurrence of a thermally induced OBDD−OBDG OOT in a sPP-*b*-PS diblock copolymer. Although such a phase transition has not been found for diblock copolymers previously, Benedicto et al. have mathematically described one possible transformation route from D surface (in the OBDD phase) into G surface (in the OBDG phase) on the basis of a continuous homotopic transformation through the minimal surfaces;[38] namely, the transformation from (6,4) net of D surface into (10,3) net of G surface can be achieved by "randomly pulling apart" a tetrahedral vertex to form two trigonal vertices. It is noted that pulling all vertices apart in one direction would result in the *Fddd*-type (10,3) net structure. However, the possibility of the *Fddd* structure has already been ruled out for the present diblock in conjunction with Figure 1b.

Here we would like to further discuss the thermodynamic driving forces that control the formation of the OBDD and OBDG phases in response to the temperature change. The main difference between the elementary units of the two bicontinuous structures lies in the degree of packing frustration associated with the stretching of the minority block chains (i.e., sPP blocks in our diblock), where the minority block chains have to be stretched more to fill the space at the center of the four-connector (in the OBDD structure) than that of the three-connector (in the OBDG structure). On the other hand, the four-connector domain in OBDD has a lower surface area per unit volume than that of the three-connector in gyroid[39] and should hence suffer a lower interfacial energy. Nevertheless, the enthalpy difference between surfaces "G" and "D" was calculated to be small when adopting an isometric mapping of minimal surface.[40,41] Since the theoretical works normally assume the block chains to obey Gaussian statistics, the relief of the entropic penalty arising from packing frustration can easily outweigh the reduction of interfacial free energy; as a result, OBDG is always predicted to be a more stable structure than OBDD for the conventional diblock copolymers even in the case of the larger segregation strength (or at lower temperatures).

Even in sPP-*b*-PS, the relief of packing frustration dominated the self-assembly, and hence the OBDG structure was favored at the high temperatures. Then why is OBDD favored for sPP-*b*-PS at the low temperatures? We may envision the following two possible physical factors: (1) a new factor involving the stereoregularity of sPP and (2) a physical factor associated with the polydispersity of sPP. We propose that factor (1) is primarily responsible for the stability of the OBDD structure; that is, the increasing degree of conformational order due to increasing amount of helical segments[42,43] of sPP block chains with lowering temperature increases the free energy release accompanied by the local packing of these segments and hence stabilizes the OBDD structure. Below we will first discuss factor (1) and then factor (2).

Stereoregular polymers such as iPP, sPP, iPS, and sPS adopt helical conformation in the crystalline state.[44−47] The helical segments however do not completely disappear even above the crystal melting point. In the case of sPP, the helical conformation of the segments in the noncrystalline state (H_A) gives rise to absorption peaks at 977, 844, and 836 cm^{-1} in the infrared spectrum.[48] Figure 4 displays the temperature-dependent FTIR spectra of the diblock to examine the existence of helical segments in sPP block and the temperature dependence of their population (the entire spectrum is shown in Figure S9 of the Supporting Information). Since the argument that the formation of the OBDD structure in the sPP-*b*-PS may be associated with the crystallization of sPP blocks could be precluded due to the existence of OBDD even in the melt state, we consider the conformation of sPP in the melt state only. As shown in Figure 4, the population of H_A decreased with raising temperature across the OBDD-to-OBDG transition temperature, as manifested by comparing the spectrum collected at 140 °C to that obtained at 175 °C, and this tendency was continuous to 200 °C. Upon cooling, the H_A signal was recovered.

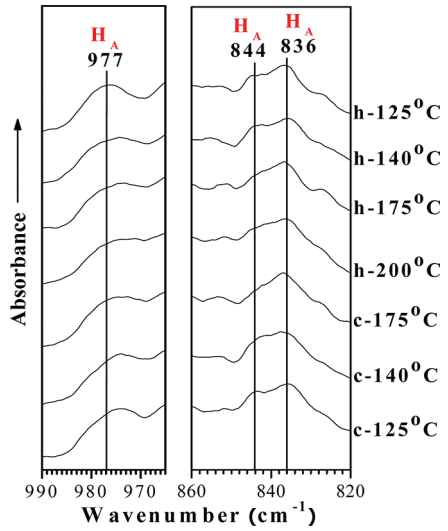

Figure 4. Temperature-dependent FTIR spectra of sPP-*b*-PS, in which "H_A" denotes the signals of helical chain conformation of sPP blocks at 977, 844, and 836 cm^{-1} in the noncrystalline state. "h" and "c" denote the spectra collected in the heating and cooling cycle, respectively. The spectra are vertically shifted to avoid overlaps.

The observed temperature dependence was analogous to that found in the previous temperature-dependent FTIR studies of the thermal stability of helical segments of sPP homopolymer in the melt state,[42,43] where the absorbance of the 977 cm^{-1} band was used as an index for the population of helical segments. It was postulated that the decrease of the helical segment population on heating was associated with the partial destruction of the longer helical segments into the shorter ones. The FTIR spectra hence confirmed that the amount of

dx.doi.org/10.1021/ma202057g | *Macromolecules* 2012, 45, 2471−2477

helical segments in sPP blocks in the OBDD phase is higher than that in the OBDG phase. When the population of helical segments was sufficiently high, their mutual interactions would allow sPP blocks to form locally ordered structures or mesomorphic packing of the helical segments. In this case, the entropic penalty associated with chain stretching was effectively compensated by the release of free energy on forming the mesomorphically ordered regions in the microdomains. The role of packing frustration, which is important for Gaussian chains, was hence greatly relaxed by locally ordered mesomorphic packing of the helical segments in the case of the block copolymer with the stereoregular block chain; as a consequence, OBDD became the favorable structure because of the lower interfacial free energy and lower free energy of the chain packing in the microdomain. The relief of packing frustration regained its dominant role when the population of helical segments was low at sufficiently high temperature, and thereby the OBDG phase became the more stable structure.

The issue for the relief of the packing frustration that dominated the self-assembly at the high temperatures of sPP-*b*-PS was further evidenced by blending with the corresponding constituent sPP homopolymer (see Figure S10 of the Supporting Information). It was found that the OBDD structure could also be formed in the sPP-*b*-PS/sPP blends. The OBDD-to-OBDG transition temperature of the blend was found to locate at ca. 10−20 °C higher than that of neat diblock, as the homopolymer chains were able to be segregated to fill the space at the center of the connectors to release the packing frustration. This thereby enhanced the stability of OBDD phase.

Let us now consider factor (2), i.e., the effect of the polydispersity of sPP (PDIs of sPP and PS blocks in our block copolymer are 1.32 and 1.02, respectively) on the stabilization of OBDD. If the polydispersity is caused by a contamination with sPP homopolymer, the sPP homopolymer can stabilize the OBDD as elucidated immediately above. However, we can rule out this possibility of the homopolymer contamination evidently from the symmetric GPC elution curve (see Figure S2 of the Supporting Information). Thus, we can focus on the issue whether the polydispersity of sPP-*b*-PS would stabilize the OBDD structure. Generally, the polydispersity of block copolymers varies the interface curvature and thereby the morphology of the microdomain primarily via the so-called "cosurfactant effect"[30] which is brought about by block chains having different chain lengths being packed in a given microdomain with their chemical junctions on the common interface. The effect was explored extensively for not only binary mixtures of diblock copolymers[49] but also block copolymers with polydispersity.[31,50,51] However, to our best knowledge, these copolymer systems having essentially random-coil conformation and van der Waals interactions never showed the OBDD structures; that is, their ordered bicontinuous structure reported so far is the OBDG phase. Thus, even in the block copolymers with relatively high molecular weight polydispersity, OBDG is still a selected equilibrium morphology but not OBDD, as long as the block chains adopt random-coil conformations and have van der Waals interactions only.

CONCLUSIONS

We have discovered that a slightly asymmetric sPP-*b*-PS as-cast from xylene displayed the OBDD structure. When the OBDD-forming copolymer was heated, this structure transformed into the gyroid (OBDG) phase at ca. 155 °C. Interestingly, OBDG transformed back to OBDD upon cooling. The thermal reversibility of the transformation indicated that OBDD was a thermodynamically stable structure for this system. This was in contradiction to the previous theoretical works which predicted that OBDD is unstable relative to OBDG for neat diblocks irrespective of the segregation strength, whereas OBDD may exist over a narrow window in the blend of A-*b*-B with homopolymer A. We propose that when the population of helical segments of sPP block in the melt was sufficiently high, their mutual interactions would allow sPP blocks to form locally ordered or mesomorphic packing of the helical segments. In this case, the entropic penalty associated with chain stretching was effectively compensated by the release of free energy on forming the ordered regions in the microdomains. The role of packing frustration was hence greatly relaxed and OBDD became the favorable structure.

ASSOCIATED CONTENT

Supporting Information

GPC elution curve and ^{1}H NMR spectrum of sPP-*b*-PS; theoretical SAXS profiles of the OBDD and OBDG phase; entire temperature-dependent SAXS profiles of sPP-*b*-PS; DSC heating scan of sPP-*b*-PS; SAXS profile of sPP-*b*-PS collected at room temperature after the sample has been isothermally annealed at 140 °C for 24 h; a transmission electron micrograph (TEM) of sPP-*b*-PS; entire temperature-dependent FTIR spectra of sPP-*b*-PS; SAXS profiles of neat sPP-*b*-PS and sPP-*b*-PS/sPP blends. This material is available free of charge via the Internet at http://pubs.acs.org.

AUTHOR INFORMATION

Corresponding Author

*E-mail: hlchen@che.nthu.edu.tw (H.-L.C.); hashi2@pearl.ocn.ne.jp (T.H.).

ACKNOWLEDGMENTS

We gratefully acknowledge the financial support from the National Science Council Taiwan under grant NSC 97-2221-E-007-034. We also thank the National Synchrotron Radiation Center for supporting us to carry out the SAXS experiments at beamline BL23A1 and BL17A1 under proposal 2010-3-059-1. We also thank Profs. Hirokazu Hasegawa and Mikihito Takenaka at Kyoto University for the insightful discussions and assistance in in-house SAXS experiment. The financial support from the Interchange Association Japan for sponsoring the visit of C. Y. Chu to Kyoto University to carry out the in-house SAXS experiment is also gratefully acknowledged.

REFERENCES

(1) Matsen, M. W.; Bates, F. S. *Macromolecules* **1996**, *29*, 1091.
(2) Zhao, D.; Feng, J.; Huo, Q.; Melosh, N.; Fredrickson, G. H.; Chmelka, B. F.; Stucky, G. D. *Science* **1998**, *279*, 548.
(3) Crepaldi, E. L.; Soler-lllia, Galo J. de A. A.; Grosso, D.; Cagnol, F.; Ribot, F.; Scanchez, C. *J. Am. Chem. Soc.* **2003**, *125*, 9770.
(4) Fink, Y.; Urbas, A. M.; Bawendi, B. G.; Joannopoulos, J. D.; Thomas, E. L. *J. Lightwave Technol.* **1999**, *17*, 1963.
(5) Edrington, A. C.; Urbas, A. M.; DeRege, P.; Chen, C. X.; Swager, T. M.; Hadjichristidis, N.; Xenidou, M.; Fetters, L. J.; Joannopoulos, J. D.; Fink, Y.; Thomas, E. L. *Adv. Mater.* **2001**, *13*, 421.
(6) Sundrani, D.; Sibener, S. J. *Macromolecules* **2002**, *35*, 8531.
(7) Kim, S. O.; Solak, H. H.; Stoykovich, M. P.; Ferrier, N. J.; dePablo, J. J.; Nealey, P. F. *Nature* **2003**, *424*, 411.

(8) Stoykovich, M. P.; Muller, M.; Kim, S. O.; Solak, H. H.; Edwards, E. W.; de Pablo, J. J.; Nrslry, P. F. *Science* **2005**, *308*, 1442.
(9) Hajduk, D. A.; Harper, P. E.; Gruner, S. M.; Honeker, C. C.; Kim, G.; Thomas, E. L.; Fetters, L. J. *Macromolecules* **1994**, *27*, 4063.
(10) (a) Hashimoto, T.; Tsutsumi, K.; Funaki, Y. *Langmuir* **1997**, *13*, 6869. (b) Hashimoto, T.; Nisikawa, Y.; Tsutsumi, K. *Macromolecules* **2007**, *40*, 1066.
(11) Okumura, A.; Nishikawa, Y.; Hashimoto, T. *Polymer* **2006**, *47*, 7805.
(12) Urbas, A. M.; Maldovan, M.; DeRege, P.; Thomas, E. L. *Adv. Mater.* **2002**, *14*, 1850.
(13) Crossland, E. J. W.; Kamperman, M.; Nedelcu, M.; Ducati, C.; Wiesner, U.; Smilgies, D.-M.; Toombes, G. E. S.; Hillmyer, M. A.; Ludwigs, S.; Steiner, U.; Snaith, H. J. *Nano Lett.* **2009**, *9*, 2807.
(14) Liu, Z.; Li, Y.; Zhao, Z.; Cui, Y.; Hara, K.; Miyauchi, M. *J. Mater. Chem.* **2010**, *20*, 492.
(15) Hsueh, H. Y.; Chen, H. Y.; She, M. S.; Chen, C. K.; Ho, R. M.; Gwo, S.; Hasegawa, H.; Thomas, E. L. *Nano Lett.* **2010**, *10*, 4994.
(16) Thomas, E. L.; Alward, D. B.; Kinning, D. J.; Martin, D. C.; Handlin, D. L. Jr.; Fetters, L. J. *Macromolecules* **1986**, *19*, 2197.
(17) Hasegawa, H.; Tanaka, H.; Yamasaki, K.; Hashimoto, T. *Macromolecules* **1987**, *20*, 1651.
(18) Larsson, K. *J. Phys. Chem.* **1989**, *93*, 7304.
(19) Anderson, D. M.; Thomas, E. L. *Macromolecules* **1988**, *21*, 3221.
(20) Olmsted, P. D.; Milner, S. T. *Phys. Rev. Lett.* **1994**, *72*, 936.
(21) Likhtman, A. E.; Semenov, A. N. *Macromolecules* **1994**, *27*, 3103.
(22) Matsen, M. W.; Schick, M. *Phys. Rev. Lett.* **1994**, *72*, 2660.
(23) Matsen, M. W.; Schick, M. *Macromolecules* **1994**, *27*, 7157.
(24) Matsen, M. W.; Schick, M. *Macromolecules* **1994**, *27*, 6761.
(25) Thomas, E. L.; Anderson, D. M.; Henkee, C. S.; Hoffman, D. *Nature* **1988**, *334*, 598.
(26) Matsen, M. W.; Bates, F. S. *Macromolecules* **1996**, *29*, 7641.
(27) Winey, K. I.; Thomas, E. L.; Fetters, L. J. *Macromolecules* **1992**, *25*, 422.
(28) Kuo, J. C.; Tsai, J. C.; Chung, T. M.; Ho, R. M. *Macromolecules* **2006**, *39*, 7520.
(29) OBDD and OBDG normally appear at volume fraction of 0.27−0.33 for the minority component for the conventional diblock copolymers such as those composed of PS and polyisoprene or polybutadiene. Thus, the observation of OBDD and OBDG for sPP-*b*-PS with volume fraction of sPP = 0.46 is rather unique, which may be attributed to the cosurfactant effect,[30] the polydispersity effect or dissimilarity of segmental volumes of the two kinds of block copolymer chains.[31] It is noted that a PS-*b*-poly(dimethylsiloxane) was found to exhibit OBDG structure at a rather symmetric volume fraction of 0.40−0.41.[32]
(30) Hasegawa, H.; Hashimoto, T. In *Comprehensive Polymer Science, Second Supplement*; Aggarwal, S., Russo, S., Eds.; Pergamon: New York, 1996; Chapter 14, pp 497−539.
(31) Lynd, N. A.; Hillmyer, M. A. *Macromolecules* **2005**, *38*, 8803.
(32) Politakos, N.; Ntoukas, E.; Avgeropoulos, A.; Krikorian, V.; Pate, B. D.; Thomas, E. L.; Hill, R. M. *J. Polym. Sci., Part B: Polym. Phys.* **2009**, *47*, 2419.
(33) Förster, S.; Timmann, A.; Schellbah, C.; Meyer, A.; Funari, S. S.; Mulvaney, P.; Knott, R. *J. Phys. Chem. B* **2005**, *109*, 1347.
(34) Takenaka, M.; Wakada, T.; Akasaka, S.; Nishitisuji, S.; Saijo, K.; Shimizu, H.; Kim, M. I.; Hasegawa, H. *Macromolecules* **2007**, *40*, 4399.
(35) Hashimoto, T.; Koga, T.; Koga, T.; Sakamoto, N.; In *The Physics of Complex Fluids*, Yonezawa, F., Tsuji, K., Kaji, K., Doi, M., Fujiwara, T.; Eds., World Scientific: Singapore, 1998, pp 291−308.
(36) Koga, T.; Koga, T.; Hashimoto, T. *Phys. Rev. E* **1999**, *60*, R1154−R1157.
(37) Koga, T.; Koga, T.; Hashimoto, T. *J. Chem. Phys.* **1999**, *110*, 11076.
(38) Benedicto, A. D.; O'Brien, D. *Macromolecules* **1997**, *30*, 3395.
(39) Schoen, A. H. *NASA Tech. Note* **1970**, *D-5541*, 1−98.
(40) Nitsche, J. C. C. *Lectures on Minimal Surfaces*; Cambridge University Press: Cambridge, England, 1989; Vol. 1.
(41) Dierkes, U.; Hildebrandt, S.; Kuster, A.; Wohlrab, O. *Minimal Surfaces I*; Springer-Verlag: Berlin, 1992.
(42) Sevegney, M. S.; Kannan, R. M.; Siedle, A. R.; Percha, P. A. *J. Polym. Sci., Part B: Polym. Phys.* **2005**, *43*, 439.
(43) Zheng, C. X.; Zhang, X. Q.; Dong, X.; Zhao, Y.; Wang, Z. G.; Zhu, S. N.; Xu, D. F.; Wang, D. J. *Polymer* **2006**, *47*, 7813.
(44) Kobayashi, M.; Tsumura, K.; Tadokoro, H. *J. Polym. Sci., Part A: Polym. Chem.* **1968**, *6*, 1493.
(45) Lotz, B.; Lovinger, A. J.; Cais, R. E. *Macromolecules* **1988**, *21*, 2375.
(46) Brookes, A.; Dyke, J. M.; Hendra, P. J.; Meehan, S. *Spectrochim. Acta, Part A* **1997**, *53*, 2313.
(47) Rizzo, P.; Lamberti, M.; Albunia, A. R.; Ruiz de Ballesteros, O.; Guerra, G. *Macromolecules* **2002**, *35*, 5854.
(48) Sevegney, M. S.; Parthasarthy, G.; Kannan, R. M.; Thurman, D. W.; Fernandez-Ballester, L. *Macromolecules* **2003**, *36*, 6472.
(49) See for example: (a) Court, F.; Hashimoto, T. *Macromolecules* **2001**, *34*, 2536−2545. (b) Court, F.; Hashimoto, T. *Macromolecules* **2002**, *35*, 2566−2575. (c) Court, F.; Yamaguchi, D.; Hashimoto, T. *Macromolecules* **2008**, *41*, 4828−4837. (d) Hashimoto, T.; Yamaguchi, D.; Court, F. *Macromol. Symp.* **2003**, *195*, 191−200. (e) Chen, F.; Kondo, Y.; Hashimoto, T. *Macromolecules* **2007**, *40*, 3714−3723.
(50) Sides., S. W.; Fredrickson, G. H. *J. Chem. Phys.* **2004**, *121*, 4974.
(51) Cooke, D. M.; Shi, A. C. *Macromolecules* **2006**, *39*, 6661.